Title

THE 31p(t,p) 33P REACTION AMD THE USEFULNESS OF DOUBLE-STRIPPING IN DISTINGUISHING BETWEEN SHELL MODEL CALCULATIONS

Authors

Davies, W.G.
Hardy, J.C.
Darcey, W.

Publication Date

1969

UCRL-18686

THE $^{31}P(t, p)^{33}P$ REACTION AND THE USEFULNESS OF DOUBLE-STRIPPING IN DISTINGUISHING BETWEEN SHELL MODEL CALCULATIONS

W. G. Davies, J. C. Hardy, and W. Darcey

January 1969

LAWRENCE RADIATION LABORATORY
UNIVERSITY of CALIFORNIA BERKELEY

UCRL-18686

DISCLAIMER

To be submitted to Nuclear Physics

UCRL-18686
Preprint

UNIVERSITY OF CALIFORNIA

Lawrence Radiation Laboratory
Berkeley, California 94720

AEC Contract No. W-7405-eng-48

THE $^{31}P(t,p)^{33}P$ REACTION AND THE USEFULNESS OF DOUBLE-STRIPPING IN DISTINGUISHING BETWEEN SHELL MODEL CALCULATIONS

W. G. Davies, J. C. Hardy, and W. Darcey

January 1969

THE $^{31}P(t,p)^{33}P$ REACTION AND THE USEFULNESS OF DOUBLE-STRIPPING IN DISTINGUISHING BETWEEN SHELL MODEL CALCULATIONS

W. G. Davies

Nuclear Physics Laboratory, Oxford, and
Nuclear Research Center
The University of Alberta
Edmonton, Alberta, Canada†

J. C. Hardy

Nuclear Physics Laboratory, Oxford, and
Lawrence Radiation Laboratory, Berkeley, California††

and

W. Darcey

Nuclear Physics Laboratory, Oxford

Abstract

The reaction $^{31}P(t,p)^{33}P$ has been used to identify the ground state and 18 excited states of ^{33}P. The L-values of the neutron-pairs transferred to seven of the levels were determined, and spectroscopic arguments used to assign spins and parities. Shell model calculations have been carried out using five sets of two-body interaction matrix elements, and the results were compared to the observed relative peak cross sections. The same calculations were also used in a discussion of the reaction $^{34}S(d,^{3}He)^{33}P$ and the β^{+}-decay of ^{33}Ar to $T = \frac{3}{2}$ levels in ^{33}Cl. The sensitivity of the two-nucleon transfer reaction to small differences in the calculated wave functions is emphasized.

---

†Present address: Chalk River Nuclear Laboratories, Chalk River, Ontario.

††Present address: Lawrence Radiation Laboratory, Berkeley, California.

NUCLEAR REACTIONS $^{31}P(t,p)E_t$ = 12.1 MeV; measured $\sigma(E_p,\theta)$ ^{33}P deduced levels, J, π, L.

Natural target

1. Introduction

The (t,p) reaction has already been used[1]) in the $(2s_{1/2}, 1d_{3/2})$ shell to investigate some of the consequences of existing shell-model calculations[2,3,4]). A particularly simple case was chosen, the target being the "core" nucleus ^{28}Si, in order to single out the effects of particular two-body matrix elements. Since the differential cross-section for a two-nucleon transfer reaction depends critically upon the signs as well as magnitudes of shell-model components in the nuclear wave functions, the signs of two matrix elements could be uniquely determined. It is now of interest to investigate the same reaction on nuclei whose wave functions depend not just on the choice of a few two-body matrix elements, but on that of all 15 matrix elements (and 2 single-particle binding energies) necessary to specify the entire shell. There have been a number of determinations of these matrix elements using various criteria[1,2,3,4]), all of which lead to similar fits to experimental energy levels. It is then particularly valuable to have an additional sensitive test of the relative merits of these calculations.

The experiment chosen for this purpose was $^{31}P(t,p)^{33}P$. The nuclei involved have enough active particles that their wave functions depend upon all matrix elements, and there is the additional advantage that none of the levels in ^{33}P were used in the original determination of the matrix-element values, thus providing an independent assessment.

As an additional source of spectroscopic information, as well as underlining the value of the two-nucleon data, calculations are presented for the reaction $^{34}S(d,^{3}He)^{33}P$ and the β^{+}-decay of the mirror nucleus ^{33}Ar to $T = \frac{3}{2}$ states in ^{33}Cl.

2. Theory

2.1. THE (t,p) REACTION

The differential cross-section of the reaction A(t,p)B can be described using the distorted wave Born approximation (DWBA). If the interaction is assumed to have zero range, and the effects of spin-orbit coupling in the optical potentials are neglected, the following expression is obtained[5]):

$$\frac{d\sigma}{d\Omega} = \frac{\mu_p \mu_t}{(2\pi\hbar^2)^2} \cdot \frac{k_p}{k_t} \cdot \frac{(2J_B+1)}{(2J_A+1)} \sum_{\Lambda}^{LSJT} b_{ST}^2 \, (T_A N_A TN | T_B N_B)$$

$$\times \left| \sum^{\rho_1 \rho_2} \left(2-\delta_{\rho_1,\rho_2}\right)^{1/2} \mathcal{S}_{AB}^{1/2}(\rho_1\rho_2, JT) \begin{bmatrix} \ell_1 & \ell_2 & L \\ 1/2 & 1/2 & S \\ j_1 & j_2 & J \end{bmatrix} \right.$$

$$\left. \sum^{\ell_a \ell_b} \Gamma^{L\Lambda}_{\ell_a \ell_b} \, P_{\ell_b \Lambda}(\cos\theta) \, \mathcal{J}^{\ell_1 \ell_2 L \ell_a \ell_b} \right|^2 \qquad (1)$$

where μ and k are the reduced mass and wave number of the light particles,

$L(\Lambda)$, S, J and T are the quantum numbers of the transferred pair of neutrons;

b_{ST} is essentially an overlap factor for the light particles, and in the case of the (t,p) reaction it equals $\delta_{S,0}\,\delta_{T,1}$.

$\mathcal{S}_{AB}^{1/2}(\rho_1\rho_2;JT)$, the "spectroscopic amplitude," is related to the probability that the nucleons common to A and B have identical configurations in both, and that the two additional

nucleons in B have shell-model configurations denoted by $\rho_1(\equiv[n_1 \ell_1 j_1])$ and $\rho_2(\equiv[n_2 \ell_2 j_2])$. In general, configuration mixing in the wave functions of A and B introduces a coherent sum over all such possibilities.

$\begin{Bmatrix} \ell_1 & \ell_2 & L \\ 1/2 & 1/2 & S \\ j_1 & j_2 & J \end{Bmatrix}$ is the normalized 9-j symbol required to transform from j-j to LS coupling.

$\Gamma^{L\Lambda}_{\ell_a \ell_b}$ is the same function as that defined by Austern et al.[6]) and is given by:

$$\Gamma^{L\Lambda}_{\ell_a \ell_b} = i^{\ell_a - \ell_b - L} \left[\frac{(2\ell_a+1)(2\ell_b+1)}{(2L+1)}\right]\left[\frac{(\ell_b-\Lambda)!}{(\ell_b+\Lambda)!}\right]^{1/2} (\ell_a 0 \ell_b 0 | L0)(\ell_a 0 \ell_b \Lambda | L\Lambda) \tag{2}$$

$\mathcal{J}^{\ell_1 \ell_2 L \ell_a \ell_b}$ is an integral over the partial waves and the form factor of the reaction:

$$\mathcal{J}^{\ell_1 \ell_2 L \ell_a \ell_b} = \frac{B}{A k_p k_t} \int U_{\ell_b}(k_t, r)\ \mathcal{J}^{\ell_1 \ell_2 L}(r) U_{\ell_a}(k_p, \tfrac{A}{B} r) dr \ . \tag{3}$$

In order to explicitly evaluate this radial integral, a choice must be made for the form of the wave function of the triton, as well as that of the captured neutrons bound in the residual nucleus. Two possible choices will be considered here. The first assumes that the triton wave function may be represented by a delta function[7]), and that the bound neutrons are captured as independent particles in a Saxon-Woods well[8]). This is often called the "point triton" approximation (PT) and yields the following expression[5]):

$$\mathcal{F}_{PT}^{\ell_1 \ell_2 L}(r) = D_0 \, i^{\ell_1+\ell_2-L} \left[\frac{(2\ell_1+1)(2\ell_2+1)}{(2L+1)}\right]^{1/2} (\ell_1 0 \ell_2 | L0)$$

$$\frac{U^{[n_1 \ell_1 j_1]}(r)}{r} \quad \frac{U^{[n_2 \ell_2 j_2]}(r)}{r} \tag{4}$$

where D_0 is the zero-range constant, and the single-particle wave functions were taken to be

$$\phi_\lambda^{[n\ell j]}(r) = \frac{U^{[n\ell j]}(r)}{r} \; [i^\ell \, Y_{\ell\lambda}(\hat{\underline{r}})] \tag{5}$$

The second choice assumes that the triton wave function has a Gaussian form[9]) and the single-particle wave functions are given by:

$$\phi_\lambda^{[n\ell j]}(\underline{r}) = R_{\bar{n}\ell}(\nu r^2) \; [i^\ell \, Y_{\ell\lambda}(\hat{\underline{r}})] \tag{6}$$

where $\bar{n} = n-1$, and $R_{\bar{n}\ell}$ is the radial part of the usual harmonic oscillator wave function[10]). We shall refer to this as the "zero-range interaction" approximation (ZI). The form factor, corresponding to equation (4), is[5]):

$$\mathcal{F}_{ZI}^{\ell_1 \ell_2 L}(r) = \sqrt{4\pi} \; C_0 \, i^{\ell_1+\ell_2-L} \sum^{nN} \langle \bar{n}0\bar{N}L:L | \bar{n}_1 \ell_1 \bar{n}_2 \ell_2 : L \rangle \; \Omega_n \; R_{\bar{N}L}(2\nu r^2) \tag{7}$$

where $\langle \; | \; \rangle$ is a Moshinsky transformation bracket[11]), and Ωn results from integration over the relative coordinates of the transferred neutrons; Ωn has been evaluated in ref. [9]).

As indicated for the PT approximation, the radial wave functions of the captured nucleons are taken to be eigenfunctions of a Saxon-Woods potential, since such wave functions exhibit an asymptotic behaviour which corresponds to some binding energy. In practice, the well-depth is adjusted for both wave functions to make the binding energy of each nucleon equal to half the observed separation energy. On the other hand, the harmonic oscillator wave function used in the ZI approximation does not have the correct asymptotic form. To correct for this, it is matched at some suitably large radius to a Hankel function corresponding to the total observed separation energy[9]).

The PT and ZI approximations are expected to give very similar predictions at least in cases, such as those considered here, where the ℓ-values of the transferred nucleons are not too different. It will be seen in what follows (where $\ell=0$ and 2) that this is correct.

2.2. SHELL MODEL CALCULATION

In writing the single particle wave functions as in equations (5) and (6), we have tacitly assumed spherical symmetry. In accord with this assumption we shall adopt the intermediate-coupling shell-model, and generate nuclear wave functions for A(^{31}P) and B(^{33}P) from which the spectroscopic amplitudes can be calculated.

The details of the shell-model calculations that will be used here are similar to those described by Glaudemans et al.[2]). Our model assumes ^{28}Si to be an inert core, and considers the additional active nucleons to be in the $2s_{1/2}$ and $1d_{3/2}$ shells. The residual interactions between these active nucleons can be expressed as linear combinations of two-body-interaction matrix elements. If the relevant wave functions for the nuclei involved

are written as

$$\psi_{\Gamma_A} = \sum_i a_i \psi(s^{n_i} \alpha_i, d^{m_i} \beta_i; \Gamma_A)$$

$$\psi_{\Gamma_B} = \sum_j b_j \psi(s^{n_j} \gamma_j, d^{m_j} \delta_j; \Gamma_B) \qquad (8)$$

then the coefficients a_i (or b_j) are components of an eigenvector of the N-body Hamiltonian, where $N = n_i + m_i$ (or $n_j + m_j$). The notation used in equation (8), and in subsequent equations, is similar to that of Macfarlane and French[12]). The symbols s^n and d^m indicate n-particles in the $2s_{1/2}$ shell and m-particles in the $1d_{3/2}$ shell; the Greek letters α and β (γ and δ) denote all quantum numbers which are necessary to specify the state of those particles in the $2s_{1/2}$ and $1d_{3/2}$ shell respectively. The quantum numbers of the complete nuclear wave functions are represented by Γ_A and Γ_B.

All wave functions describing nuclei with active nucleons in these two shells can now be computed from a knowledge of seventeen parameters, fifteen two-body-interaction matrix elements and two single particle binding energies. There are three possible methods for determining the values of the parameters:

1) they may be calculated directly from first principles assuming a particular form for the nucleon-nucleon interaction;

2) they may be calculated by choosing an interaction potential which involves a restricted number of free parameters, the values of which being

determined from a least-squares fit of the energy eigenvalues to certain experimental energy levels;

or 3) all seventeen parameters may be treated as free, and optimum values determined from a similar least-squares fit.

Five sets of matrix elements will be used in the present calculations, and these are listed in table 1. The criteria used in their determination will be discussed individually.

Set I: These matrix elements were evaluated using method 3) where a least-squares fit was obtained[3]) to the binding energies of 50 selected levels in nuclei between ^{28}Si and ^{40}Ca.

Set II: An analysis of the reaction ^{28}Si(t,p)^{30}Si indicated[1]) that the sign of $\langle s^2|V|d^2\rangle_{01}$ had been incorrectly chosen in ref. [3]). Set II is identical to Set I except that this sign has been changed, and as such it is unoptimized in the sense that it was not fitted to data throughout the entire shell. It is introduced solely to show the affect of the sign change. The following set also uses the sign change but it has been optimized; there are no large discrepancies between the two.

Set III: The method used was the same as that for Set I except that the binding energies of 60 levels were utilized in the fit[4]). The sign of $\langle s^2|V|d^2\rangle_{01}$ was the same as in Set II.

Set IV: Method 3) was again used, but in this case the excitation energies, rather than the binding energies, of 35 levels were considered.

Set V: The surface delta interaction (SDI) was employed to express all two-body matrix elements in terms of two parameters: the strengths of the (S=0) and (S=1) interactions[4,13]). Method 2) was then used to determine these parameters by fitting excitation energies[4]).

2.3. CALCULATION OF SPECTROSCOPIC AMPLITUDES

For the reaction A(t,p)B we shall consider the wave functions of A and B are those given by equation (8). Spectroscopic amplitudes can be readily calculated for states described by such shell model wave functions[5]). There are three possible ways of transferring two nucleons into the $2s_{1/2}$ and $1d_{3/2}$ shells, and the explicit equations for the relevant spectroscopic amplitudes are:

$$\mathcal{S}^{1/2}_{AB}(s^2;\Gamma) = \sum_{ij} a_i b_j (-1)^{\Gamma_B-\Gamma_A-\gamma_j+\alpha_i} \left(\frac{n_j(n_j-1)}{2}\right)^{1/2} \langle s^{n_j}\gamma_j\{|s^{n_j-2}\alpha_i;s^2\Gamma\rangle$$

$$\times\ U(\delta_j\alpha_i\Gamma_B\Gamma;\Gamma_A\gamma_j)\ \delta_{m_i,m_j}\ \delta_{n_i+2,n_j}\ \delta_{\beta_i,\delta_j}$$

$$\mathcal{S}^{1/2}_{AB}(sd,\Gamma) = \sum_{ij} a_i b_j (-1)^{m_j-1} (n_j m_j)^{1/2} \langle s^{n_j}\gamma_j\{|s^{n_j-1}\alpha_i\rangle\langle d^{m_j}\delta_j\{|d^{m_j-1}\beta_i\rangle$$

$$\times \begin{Bmatrix} \alpha_i & s & \gamma_j \\ \beta_i & d & \delta_j \\ \Gamma_A & \Gamma & \Gamma_B \end{Bmatrix} \delta_{n_i+1,n_j}\ \delta_{m_i+1,m_j}$$

$$\mathcal{S}^{1/2}_{AB}(d^2;\Gamma) = \sum_{ij} a_i b_j \left(\frac{m_j(m_j-1)}{2}\right)^{1/2} \langle d^{m_i}\delta_j\{|d^{m_j-2}\beta_i;d^2\Gamma\rangle$$

$$\times\ U(\gamma_j\beta_i\Gamma_B\Gamma;\Gamma_A\delta_j)\ \delta_{n_i,n_j}\ \delta_{m_i+2,m_j}\ \delta_{\alpha_i,\gamma_j} \qquad (9)$$

In the interpretation of these equations, the normalized Racah coefficients. U, and the normalized 9-j symbols [ ], with Greek letter arguments, should be written as product pairs in J and T. For example,

$$U(\alpha_1\alpha_2\alpha_3\alpha_4;\alpha_5\alpha_6) \equiv U(J_1J_2J_3J_4;J_5J_6)U(T_1T_2T_3T_4;T_5T_6)$$

Also $$(-1)^{\alpha} \equiv (-1)^{J+T}$$

2.4. CALCULATION OF β-DECAY TRANSITION RATES

The ft-value for β-transition is, in general, given by the relation[14]):

$$ft = \frac{2\pi^3(\ell n 2)(\hbar^7/m_0^5c^4)}{g_v^2\langle \underline{1}\rangle^2 + g_A^2\langle \underline{\sigma}\rangle^2} = \frac{6.2 \times 10^3}{\langle \underline{1}\rangle^2 + 1.41\,\langle \underline{\sigma}\rangle^2} \text{ sec} \qquad (10)$$

where g_v and g_A are the vector and axial-vector coupling constants and the Fermi and Gamov-Teller matrix elements have been denoted by $\langle \underline{1}\rangle$ and $\langle \underline{\sigma}\rangle$. For the transition $A \xrightarrow{\beta} B$, where the wave functions are again written as in equation (8), the matrix elements can be evaluated from the following equations[14,15]):

$$\langle \underline{1}\rangle^2 = [T_A(T_A+1) - T_{ZA}T_{ZB}]\,\delta_{J_A,J_B}\,\delta_{T_A,T_B}$$

$$\langle \sigma\rangle^2 = \frac{1}{2J_A+1}\sum_{M_AM_B}\left|\sum_{ij} a_ib_j\langle s^{n_j}\gamma_j, d^{m_j}\delta_j;\Gamma_B\right|$$

$$\times \sum_{r=1}^{(n_i+m_i)} \underline{\sigma}(r)\tau_y(r)\left| s^{n_i}\alpha_i, d^{m_i}\beta_i;\Gamma_A\rangle\right|^2 \qquad (11)$$

The Gamow-Teller matrix element can be expressed as a sum over one-body matrix elements;

$$\langle\sigma\rangle^2 = \frac{1}{2J_A+1} \begin{pmatrix} T_B & 1 & T_A \\ T_{zB} & T_z & T_{zA} \end{pmatrix}^2 \left| \sum_{ijr} a_i b_j \langle U^1_{\rho_r\rho_r}\rangle \langle\rho_r\|\sigma\tau\|\rho_r\rangle \right|^2$$

where

$$\langle U^1_{ss}\rangle = n_j \left[\frac{(2\Gamma_A+1)(2\gamma_j+1)}{(2s+1)(2\alpha_i+1)} \right]^{1/2} U(\gamma_j\delta_j 1\Gamma_A;\Gamma_B\alpha_i)$$

$$\times \sum_{\eta} U(\eta\gamma_j s1;s\alpha_i)\, \langle s^{n_j}\gamma_j\{|s^{n_j-1}\eta\rangle\, \langle s^{n_j}\alpha_i\{|s^{n_j-1}\eta\rangle$$

and

$$\langle U^1_{dd}\rangle = m_j \left| \frac{(2\Gamma_B+1)}{(2d+1)} \right|^{1/2} U(\Gamma_B\gamma_j 1\beta_i;\delta_j\Gamma_A)$$

$$\times \sum_{\eta} U(\eta\delta_j d1;d\beta_i)\, \langle d^{m_j}\delta_j\{|d^{m_j-1}\eta\rangle\, \langle d^{m_j}\beta_i\{|d^{m_j-1}\eta\rangle$$

The one-body matrix elements $\langle\rho_r\|\sigma\tau\|\rho_r\rangle$ have the values

$$\langle s\|\sigma\tau\|s\rangle = 6$$

and $$\langle d\|\sigma\tau\|d\rangle = -6\sqrt{2/5} \quad .$$

3. Experimental Procedure and Results

The $^{31}P(t,p)^{33}P$ experiment was performed with 12.1 MeV incident tritons from the A.W.R.E. (Aldermaston) Tandem Van de Graaff. The emitted protons were recorded on "Ilford K-2" nuclear emulsions placed in the focal planes of the 24-gap magnetic spectrograph[16]). The phosphorus target was ~ 300 $\mu gm/cm^2$ thick, vacuum evaporated on a 10 $\mu gm/cm^2$ carbon backing. Figure 1 shows the energy spectrum recorded at 27.5° for a 3000 μC exposure, where the energy range covered includes all levels in ^{33}P up to 5.8 MeV excitation.

Angular distributions of those proton groups which corresponded to levels below 5 MeV and appeared to be predominantly stripping in character are displayed in fig. 2. The curves shown in the figure were computed using both the PT and ZI approximations. The program used for the PT calculations was coded by M. J. L. Yates, while that used in the ZI calculation was based on DWUCK (coded by P. D. Kunz) and modified by us.† The parameters used for the computations are given in table 2. The triton parameters were interpolated from the elastic scattering results[17]) for 12 MeV tritons on ^{27}Al and ^{35}Cl, while those for protons were taken[8]) from 17.6 MeV data on ^{27}Al.

The energies of the observed levels along with the L-values giving best fit to the data are listed in table 3 together with the results of Bearse et al.[18]), Currie and Evans[19]), and Moss et al.[20]).

---

†We should like to acknowledge M. J. L. Yates and P. D. Kunz for making their programs available.

4. Analysis

4.1. THE REACTION $^{31}P(t,p)^{33}P$

An energy level diagram corresponding to the experimentally observed levels up to 5.0 MeV of excitation is shown on the left of fig. 3. Also shown in the figure are the results of shell model calculations using the five sets of matrix elements listed in table 1 and described in section 2.2. All calculations give the same sequence for the lower excited states, and it is evident that each produces an acceptable fit to the level spacings, although Set IV appears to give the best overall agreement. It is perhaps not surprising that all sets give similar adequate agreement to energy level data, since it is just such data that was used originally in determining values for the matrix elements. However, it should be noted that no levels in ^{33}P, other than the ground state, were used in any of the matrix element determinations. It will now be of interest to investigate in more detail the validity of the calculated wave functions; and for this purpose we shall examine not only the double-stripping data reported here, but also the proton pick-up experiment of Bearse et al.[18]) and the β-decay transition rates[21,22]) from the mirror nucleus ^{33}Ar.

The first step towards comparing the calculations with the (t,p) experiment is to establish the identity of the levels observed. From the L-values of the observed transitions (listed in table 3), it is possible to restrict the ground state to $\frac{1}{2}^+$ and the first three excited states to $\frac{3}{2}^+$ or $\frac{5}{2}^+$. It seems reasonable, then, initially to associate these levels with the sequence in the calculations, i.e. $\frac{1}{2}^+$, $\frac{3}{2}^+$, $\frac{5}{2}^+$, $\frac{3}{2}^+$. In table 4 we compare the experimentally observed relative peak intensities with those

obtained using DWBA computations and the PT approximation. Again the five sets of matrix elements were employed in calculating the spectroscopic amplitudes. However, here additional ambiguities arise. For calculations involving the effective interaction matrix elements (Sets I-IV) the relative sign of the s and d single-particle radial wave functions is undefined, even though the signs of the matrix elements $\langle sd|V|d^2\rangle$ and $\langle s^2|V|sd\rangle$ may have been specified.† Consequently, for each of Sets I-IV, two separate calculations of the relative peak intensities were made, corresponding to the two possible choices of relative signs. The calculations denoted by "a" assumed that all single particle wave functions were positive asymptotically, while those denoted by "b" made the opposite choice for the relative signs.

In the derivation of the matrix elements for the Surface Delta Interaction (Set V) the interaction potential was defined to be attractive[13]) and it was assumed that "the radial one-particle wave functions of the active shells all have approximately the same form and amplitude at the nuclear surface"[4]). Since there is good evidence[5]) that the (t,p) reaction is predominantly sensitive to the radial wave functions in the surface and external

†An ambiguity with an equivalent effect is the order of coupling ℓ and s to give j; this is also unspecified in a shell model calculation involving only the $1d_{3/2}$ and $2s_{1/2}$ shells.

regions, the convention chosen for the wave functions in the DWBA was that each should be positive asymptotically. However, the definition of the spherical Harmonics used in ref. [13]) did not include the factor i^{ℓ}, as in equations (5) and (6), and the appropriate changes were made in our calculations.

It can be readily seen from table 4 that dramatically different results are predicted by using the various sets of two-body matrix elements and sign conventions. However, it is important to note that all of the sets used (except IIa) predict peak cross sections which are inconsistent with the inverse identification for the first two excited states. Consequently, we shall assign $(\frac{3}{2})^+$ to the 1.427 MeV state and $(\frac{5}{2})^+$ to the 1.845 MeV state.†

The results of a similar calculation, in which the ZI approximation was used, are shown in table 5. Evidently, the different approximation used makes little essential change in the conclusions, and it is apparent from both tables 4 and 5 that the best overall agreement with the data is produced by Sets IVb and V. Using these matrix-element sets, relative intensities have been calculated for all additional states predicted to be below 5 MeV, and the results are listed in table 6. Since both the PT and ZI approximations in this application give similar results, only the former was used in this table. Above the third excited state no other positive-parity states are predicted to be strongly excited and this is confirmed by the data on table 3.

---

†The same tentative assignment was made in ref. [18]) and has been confirmed recently by Moss et al.[22]).

It is not possible on the basis of predicted intensities to determine the spin-parity of the state at 3.272 MeV beyond the restriction to $(\frac{3}{2}^+, \frac{5}{2}^+)$ imposed by its probable L-value.

It should be pointed out that the calculated results in tables 4-6 used the bound-state parameters $r=1.3$ and $a=0.6$ for the PT calculations and $\nu=0.318$ for the ZI calculations. All calculated results in these tables are relatively insensitive to changes in the optical model parameters.

Included in the experimental results in table 3 are two additional strong levels whose configurations are beyond the scope of our calculations. The state at 4.218 MeV is populated by an $L=3$ transition which restricts its spin-parity to $\frac{5}{2}^-$ or $\frac{7}{2}^-$. Since this state is presumably the lowest negative-parity state in ^{33}P, its spin-parity is probably $\frac{7}{2}^-$, representing the excitation of a single nucleon into the $(1f_{7/2})$-shell. This assignment is corroborated by the fact that the first negative-parity state in ^{31}P is $\frac{7}{2}^-$ and lies at an excitation energy of 4.431 MeV. A strong $L=0$ transition is also observed to a state at 5.650 MeV indicating that the predominate configuration of this state presumably corresponds to the excitation of two paired nucleons into the $(1f_{7/2})$-shell.

4.2. THE REACTION $^{34}S(d,^{3}He)^{33}P$

For comparison, the calculated spectroscopic factors for the reaction $^{34}S(d,^{3}He)^{33}P$ are shown in table 7. These values are considerably less sensitive to the choice of matrix elements than were the comparable calculations for the (t,p) reaction. (Of course, for single-nucleon transfer reactions the ambiguity in the relative signs of the radial wave functions is no longer important.) Although the available experimental evidence[18]) is incomplete, including only the ground and second excited state, it is unlikely that more detailed information would enable a judgment to be made of the relative merits of the various calculations. Certainly, the ground state spectroscopic factors are all roughly equivalent and are in reasonable agreement with the experimental value of 1.8.

The observation of a relatively large cross section for the pick-up reaction to the $\frac{5^+}{2}$ state at 1.845 MeV[18]) may be taken as evidence that there is some contribution from $(1d_{5/2})$-hole configurations particularly in this state. These configurations are omitted from our calculations, but are not expected to change significantly the results in tables 4-6 since $(1d_{5/2})$-hole admixtures in the $\frac{1^+}{2}$ ground state of ^{31}P are expected to be very small. The effect of such admixtures in states in ^{33}P would consequently be to reduce somewhat the calculated differential cross-section for production of these states from the (t,p) reaction, thus improving the agreement already noted in tables 4 and 5.

4.3. THE β-DECAY OF ^{33}Ar

Since ^{33}Ar is the mirror of ^{33}P, its β-decay to $T = \frac{3}{2}$ levels in ^{33}Cl involves wave functions that are identical to those already calculated for ^{33}P. In studies of delayed protons[21,22] following the decay of ^{33}Ar, the lowest $T = \frac{3}{2}$ analogue level was identified in ^{33}Cl. In addition to a super-allowed β^+-decay branch to this level, three other branches were observed leading to states at higher excitation energy in ^{33}Cl than the analogue level. The strength of these branches suggested that some, if not all, also led to $T = \frac{3}{2}$ states. In table 8 the states of interest in ^{33}Cl are listed, together with the experimental log ft values (normalized to a value of 3.2 for the analogue transition). It is clear that the 6.22 MeV state in ^{33}Cl cannot be a $T = \frac{3}{2}$ state, but it is tempting to conclude that the 7.50 and 8.15 MeV states are. However, all the evidence encountered so far indicates that the 1.84 MeV level in ^{33}P has a spin of $(\frac{5}{2})^+$ and thus its analogue in ^{33}Cl would not be expected to be fed by an allowed β^+-transition from the $\frac{1}{2}^+$ ground state of ^{33}Ar. It is possible that the state at 8.15 MeV in ^{33}Cl is the analogue of the $(\frac{3}{2})^+$ state at 2.53 MeV in ^{33}P, but if this is so it is superficially surprising that the analogue to the $(\frac{3}{2})^+$ state at 1.43 MeV in ^{33}P is not also fed by a transition with a particularly low log ft value. In table 9 the calculated log ft values for transitions to the relevant states in ^{33}Cl are shown, where the same five sets of matrix elements were used. Although more sensitive than single stripping, it is apparent that the β^+-decay transition rates are, for the most part, relatively insensitive to this choice. It is also true that in all cases, the β^+-transition to the lowest $\frac{3}{2}^+$ state is inhibited by more than a factor of ten over that to the second $\frac{3}{2}^+$ state.

This is consistent with the identification of the 8.15 MeV state in ^{33}Cl as $(J^{\pi},T) \equiv (\frac{3}{2}^{+},\frac{3}{2})$, but certainly none of the calculations adequately explain the unusual enhancement of the β-transition to this level.

5. Conclusions

From the experimental data and calculations presented here we have attempted to conclude not only spectroscopic information about ^{33}P but also to relate this information to shell-model calculations which apply to all nuclei within the $(2s_{1/2}, 1d_{3/2})$ shells. All the calculations which we considered provided equally good agreement to energy level data but gave dramatically different predictions for transition strengths in the (t,p) reaction. The fact that this reaction proved to be such a sensitive probe of the details of the calculations seemed especially interesting when compared with calculations involving other, more common, spectroscopic tools – single nucleon transfer reactions, and β-decay. Thus, the excellent agreement between experiment and the effective-interaction shell-model calculations using matrix-element Sets IV and V is noteworthy particularly considering that there is good evidence from the $(d,{}^3He)$ reaction that at least the 1.845 MeV level contains significant admixtures of configurations which include holes in the $(1d_{5/2})$ shell. Apparently the calculations, all of which considered that shell to be closed, do account reasonably well for those parts of the wave functions which include active nucleons only in the $(2s_{1/2})$ and $(1d_{3/2})$ shells. Since the next higher shells are of opposite parity, their effects on low excited states are small. Thus if the target ground state includes little contribution from shells assumed inactive, a two-nucleon stripping reaction provides a sensitive test of the relevant components in the calculated wave functions without undue distortion from neglected components. Such would not be the case for the corresponding two-nucleon pick-up reaction.

All sets with the exception of Set V treated the 15 matrix elements and 2 single-particle energies as free parameters to be determined from fitting energy level data; by assuming a surface delta interaction Set V was expressed in terms of only three free parameters. Consequently it is remarkable that the latter reproduces energy levels throughout the shell, as well as giving specific agreement with the reaction data presented here. In addition, since our conclusions are similar to those drawn from the less-detailed analysis[1] of the reaction $^{28}Si(t,p)^{30}Si$, there is also every reason to believe that this matrix-element set (as well as Set IV) should work equally well throughout the entire region – ^{28}Si to ^{40}Ca. However, even if this is so, it is clear that calculations which also include active nucleons in the $(1d_{5/2})$-shell must be performed before pick-up data can be explained as well. For the time being, there is consolation in the fact that the existing calculations, limited as they are, can provide better agreement with experiment than might have been expected.

It is unfortunate that the only matrix-element set (I) for which wave functions have been published[3] is the one least able to explain the experimental data.

6. Acknowledgments

Two of us (W.G.D. and J.C.H.) should like to thank the National Research Council (Canada) for support in the form of Postdoctorate Overseas Fellowships; we should also like to express our appreciation for the hospitality extended to us by Professors D. H. Wilkinson and K. W. Allen of the Nuclear Physics Laboratory, Oxford. Finally we acknowledge informative discussions with Drs. S. S. M. Wong and Martin Redlich.

References

1. J. C. Hardy and I. S. Towner, Phys. Letters 25B (1967) 577
2. P. W. M. Glaudemans, G. Wiechers and P. J. Brussaard, Nucl. Phys. 56 (1964) 529
3. P. W. M. Glaudemans, G. Wiechers and P. J. Brussaard, Nucl. Phys. 56 (1964) 548
4. P. W. M. Glaudemans, B. H. Wildenthal and J. B. McGrory, Phys. Letters 21 (1966) 427
5. I. S. Towner and J. C. Hardy, to be published
6. N. Austern, R. M. Drisko, E. C. Halbert and G. R. Satchler, Phys. Rev. 133 (1964) B3
7. J. R. Rook and D. Mitra, Nucl. Phys. 51 (1964) 96
8. P. E. Hodgson, The optical model of elastic scattering (Oxford University Press, London, 1963)
9. N. K. Glendenning, Phys. Rev. 137 (1965) B102
10. P. Goldhammer, Rev. Mod. Phys. 35 (1963) 40
11. M. Moshinsky, Nucl. Phys. 13 (1959) 104 and T. A. Brody and M. Moshinsky, Tables of transformation brackets (Monografias del Instituto de Fisica, Mexico, 1960)
12. M. H. Macfarlane and J. B. French, Rev. Mod. Phys. 32 (1960) 567
13. R. Arvieu and S. A. Moszkowski, Phys. Rev. 145 (1966) 830
14. J. C. Hardy and B. Margolis, Phys. Letters 15 (1965) 276
15. G. A. P. Englebertink and P. J. Brussaard, Nucl. Phys. 76 (1966) 442
16. R. Middleton and S. Hinds, Nucl. Phys. 34 (1962) 404

17. R. N. Glover and A. D. W. Jones, Nucl. Phys. 81 (1966) 268

18. R. C. Bearse, D. H. Youngblood and J. L. Yntema, Phys. Rev. 167 (1968) 1043

19. W. M. Currie and J. E. Evans, Phys. Letters 24B (1967) 399

20. C. E. Moss, R. V. Poore, N. R. Roberson and D. R. Tilley, Phys. Rev. 174 (1968) 1333

21. J. C. Hardy and R. I. Verrall, Can. Journ. of Phys. 43 (1965) 418

22. A. M. Poszkanzer, R. McPherson, R. A. Esterlund and P. L. Reeder, Phys. Rev. 152 (1966) 995

Figure Captions

Fig. 1. Energy spectrum for the reaction $^{31}P(t,p)^{33}P$ recorded at a laboratory angle of 27.5°.

Fig. 2. Angular distributions of selected proton groups from the reaction $^{31}P(t,p)^{33}P$. The results of DWBA calculations for the indicated L values are also shown: the solid curve corresponds to the PT approximation; the dashed curve, to the ZI approximation. The optical model parameters used are given in table 2.

Fig. 3. Experimental and calculated energy level schemes for ^{33}P. The numbers in Roman numerals beneath the calculated level schemes correspond to the matrix element sets listed in table 2.

Table 1

Matrix elements† for the $2s_{1/2}$ and $1d_{3/2}$ shells in MeV

JT	Set I	II	III	IV	V
$\langle s^2\|V\|s^2\rangle 01$	- 1.35	- 1.35	- 1.3	- 1.0	- 1.1
$\langle s^2\|V\|s^2\rangle 10$	- 2.40	- 2.40	- 2.3	- 2.2	- 0.5
$\langle d^2\|V\|d^2\rangle 01$	- 2.28	- 2.28	- 2.0	- 1.8	- 2.1
$\langle d^2\|V\|d^2\rangle 21$	+ 0.16	+ 0.16	+ 0.2	+ 0.2	- 0.4
$\langle d^2\|V\|d^2\rangle 10$	- 0.92	- 0.92	- 1.5	- 1.3	- 0.6
$\langle d^2\|V\|d^2\rangle 30$	- 2.64	- 2.64	- 2.5	- 2.3	- 0.6
$\langle sd\|V\|sd\rangle 10$	- 3.86	- 3.86	- 3.6	- 3.4	- 1.0
$\langle sd\|V\|sd\rangle 11$	+ 1.79	+ 1.79	+ 1.5	+ 0.9	0
$\langle sd\|V\|sd\rangle 20$	- 1.25	- 1.25	- 1.4	- 1.5	- 0.6
$\langle sd\|V\|sd\rangle 21$	- 1.01	- 1.01	- 0.8	- 0.5	- 0.9
$\langle s^2\|V\|sd\rangle 10$	- 0.29	- 0.29	- 0.5	- 0.4	0
$\langle sd\|V\|d^2\rangle 21$	+ 0.62	+ 0.62	+ 0.6	+ 0.5	+ 0.6
$\langle sd\|V\|d^2\rangle 10$	- 0.72	- 0.72	- 0.6	- 0.6	- 0.6
$\langle s^2\|V\|d^2\rangle 01$	+ 1.49	- 1.49	- 1.5	- 1.6	- 1.5
$\langle s^2\|V\|d^2\rangle 10$	+ 0.04	+ 0.04	- 0.2	- 0.4	+ 0.3
E_s	- 8.39	- 8.39	- 8.5		
E_d	- 7.17	- 7.17	- 7.2		
$E_d - E_s$				+ 1.3	+ 1.8

†All matrix elements shown in the table are fully antisymmetric. This accounts for the discrepancies with ref. [3]).

Table 2

Optical model parameters

	U (MeV)	W_v (MeV)	a (fm)	r_o (fm)	ref.
Tritons	145.2	53.7	0.6	1.40	[16]
Protons	51.8	8.6	0.48	1.30	[8]

Table 3

Experimental Results

Level	Present Experiment Energy (keV)	L	J^π	Relative Peak Intensities	Previous Results[†] Energy (keV)
g.s.	0	0	$1/2^+$	1.000	0
1	1427 ± 15	2	$3/2^+$	0.005	1435 ± 3
2	1845 ± 15	2	$5/2^+$	0.030	1850 ± 3
3	2530 ± 15	2	$3/2^+$	0.027	2543 ± 4
4	3272 ± 15	(2)	$(3/2^+,5/2^+)$	0.002	
5	3488 ± 15			~0.001	3500 ± 8
6	3623 ± 15			~0.001	3638 ± 10
7	4044 ± 15			~0.001	
8	4218 ± 15	3	$7/2^-$	0.040	
9	4847 ± 20				
10	5039 ± 20				
11	5177 ± 20				
12	5368 ± 20				
13	5438 ± 20				
14	5485 ± 20				
15	5535 ± 20				
16	5619 ± 20				
17	5650 ± 20	0	$1/2^+$	0.170	
18	5783 ± 20				

[†] See refs. [18-20].

Table 4

Comparison of experimental relative peak cross-sections for $^{31}P(t,p)^{33}P$ with those calculated using various sets of two-body matrix elements. The distorted wave calculations assumed the PT approximation

Level Energy (MeV)	J^π	Exper-iment	Calculations using Matrix Element Set -								
			Ia	Ib	IIa	IIb	IIIa	IIIb	IVa	IVb	V
0	$1/2^+$	1.000	1.000	1.000	1.000	1.000	1.000	1.000	1.000	1.000	1.000
1.427	$3/2^+$	0.005	0.035	0.301	0.007	0.0007	0.008	0.0005	.011	.002	.005
1.845	$5/2^+$	0.030	2.559	0.315	0.003	0.068	0.013	0.067	.019	.062	.065
2.530	$3/2^+$	0.027	2.087	0.122	0.0006	0.070	0.0008	0.065	.003	.053	.061

UCRL-18585

Table 5

Comparison of experimental relative peak cross-sections for $^{31}P(t,p)^{33}P$ with those calculated using various sets of two-body matrix elements. The distorted wave calculations assumed the ZI approximation

Level Energy (MeV)	J^π	Exper-iment	Calculations using Matrix Element Set -								
			Ia	Ib	IIa	IIb	IIIa	IIIb	IVa	IVb	V
0	$1/2^+$	1.000	1.000	1.000	1.000	1.000	1.000	1.000	1.000	1.000	1.000
1.427	$3/2^+$	0.005	0.045	0.416	0.006	0.0006	0.007	0.0006	0.010	0.002	0.004
1.845	$5/2^+$	0.030	3.580	0.416	0.002	0.064	0.012	0.062	0.017	0.057	0.060
2.530	$3/2^+$	0.027	3.010	0.179	0.0004	0.066	0.0006	0.062	0.003	0.050	0.058

UCRL-18686

Table 6

Calculated relative peak intensities for all levels predicted to be below 5 MeV using the two matrix-element sets giving best fit to the data for the first three excited states. The DWBA calculations assumed the PT approximation

Level order†	J^{π}	Calculations using Matrix-Element Set-	
		IVb	V
0	$1/2^+$	1.000	1.000
1	$3/2^+$	.002	.005
2	$5/2^+$	.062	.065
3	$3/2^+$	.053	.061
4	$3/2^+$	.010	.002
5	$5/2^+$	.002	.005
6		.002	.004
7		.003	.003
8		.0007	.006
9		.0006	.002

† These numbers are not necessarily synonamous with the experimental level numbering in table 3 and fig. 1.

Table 7

Calculated absolute spectroscopic factors (C^2S) for $^{34}S(d,^3He)^{33}P$ using various sets of two-body matrix elements

Level Energies (MeV)	J^π	Calculations using Matrix Element Set -				
		I	II	III	IV	V
0	$1/2^+$	1.620	1.553	1.581	1.588	1.511
1.427	$3/2^+$	0.262	0.432	0.410	0.381	0.412
1.845	$5/2^+$	-	-	-	-	-
2.530	$3/2^+$	0.038	0.007	0.004	0.021	0.030

Table 8

Data on $^{33}Ar \xrightarrow{\beta^+} {}^{33}Cl^*(T = 3/2)$

Excitation Energy[†] in ^{33}Cl (MeV)	Relative Excitation Energy in ^{33}Cl (MeV)	Known Excitation Energy in ^{33}P (MeV)	log ft values for $^{33}Ar \xrightarrow{\beta^+} {}^{33}Cl$
5.56 ± .02	0	0	3.2
6.22 ± .03	0.66		4.5
		1.43	
7.50 ± .05	1.94	1.84	4.2
8.15 ± .07	2.59	2.53	3.8

[†]Average values from ref.[21,22]).

Table 9

Calculated log ft values for some allowed transitions in $^{33}Ar \xrightarrow{\beta^+} {}^{33}Cl^*(T = 3/2)$

Levels	J^π, T	Calculations using Matrix Element Set -				
		I	II	III	IV	V
0	$1/2^+, 3/2$	3.04	3.04	3.04	3.04	3.04
1	$3/2^+, 3/2$	11.4	8.01	6.94	6.90	7.26
2	$5/2^+, 3/2$	second forbidden				
3	$3/2^+, 3/2$	5.71	5.64	5.78	6.08	5.56

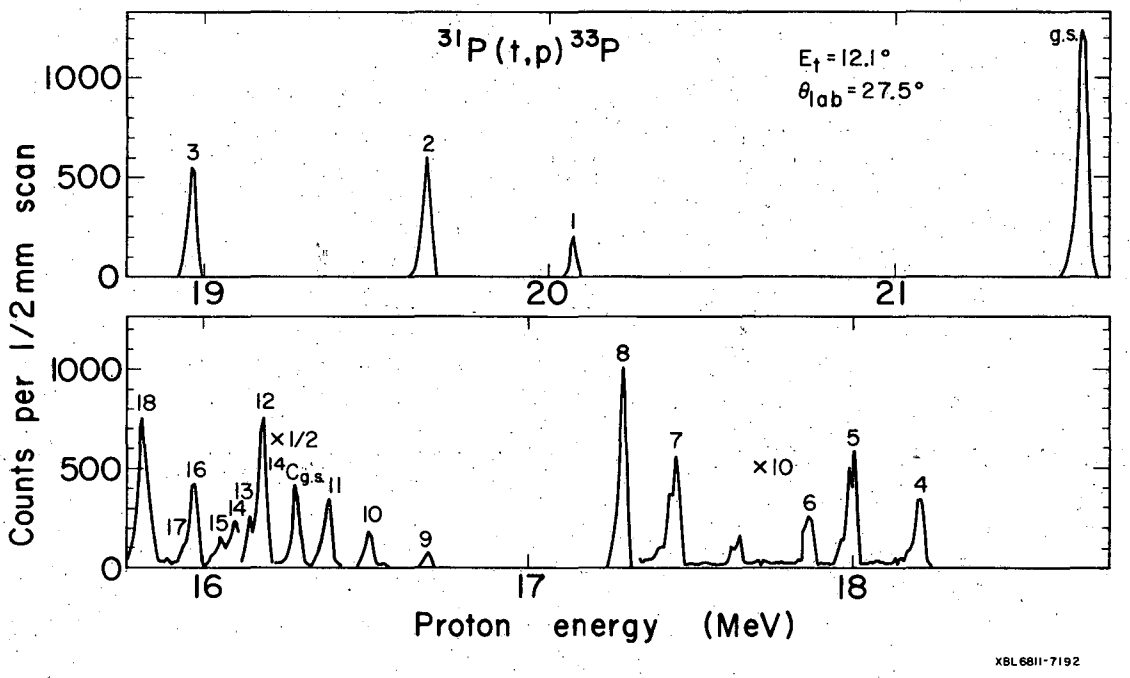
$^{31}P(t,p)^{33}P$
$E_t = 12.1°$
$\theta_{lab} = 27.5°$
g.s.
1
2
3
4
5
6
7
8
9
10
11
12
13
14
14 C g.s.
16
17
18
×1/2
×10
1000
500
0
19
20
21
16
17
18
Counts per 1/2 mm scan
Proton energy (MeV)
XBL6811-7192

Fig. 1.

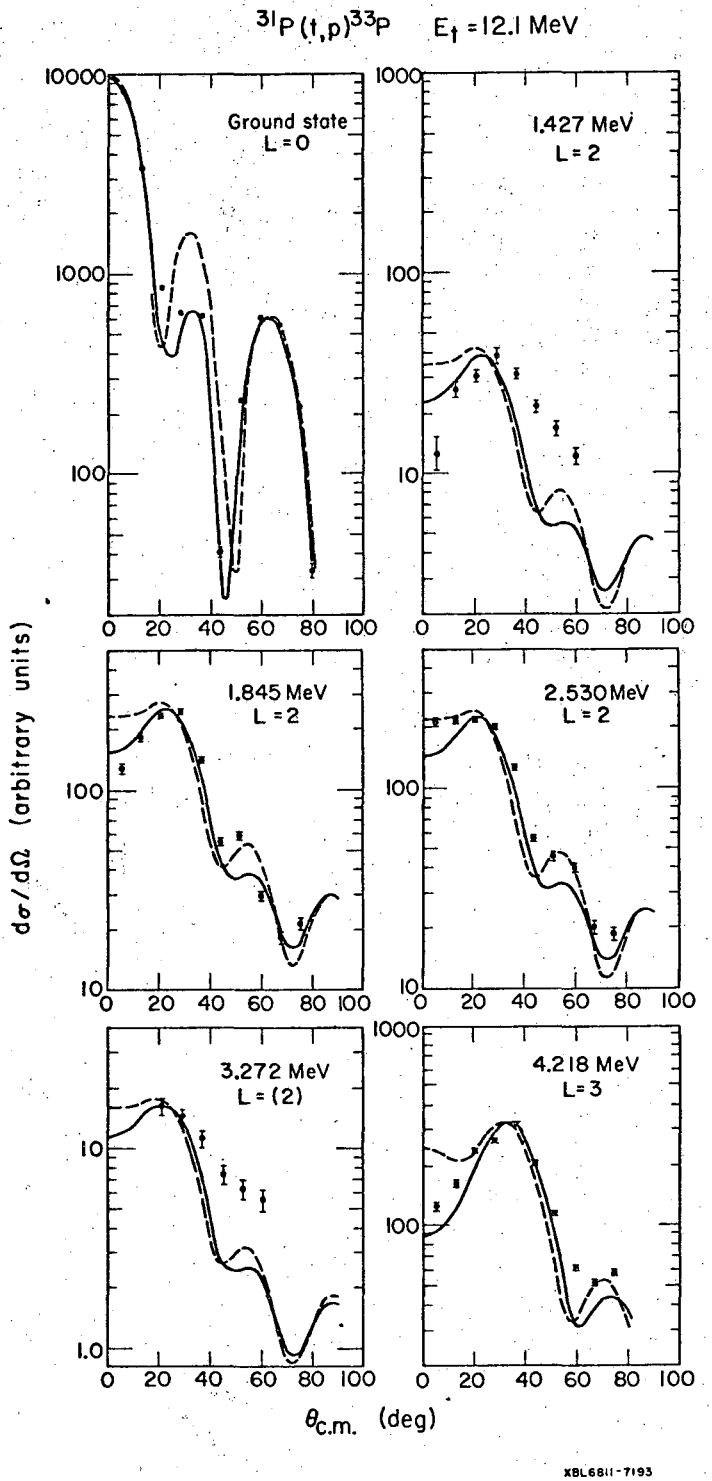
$^{31}P(t,p)^{33}P$ $E_t = 12.1$ MeV
Ground state
L = 0
1.427 MeV
L = 2
1.845 MeV
L = 2
2.530 MeV
L = 2
3.272 MeV
L = (2)
4.218 MeV
L = 3
dσ/dΩ (arbitrary units)
θc.m. (deg)
XBL6811-7193

Fig. 2.

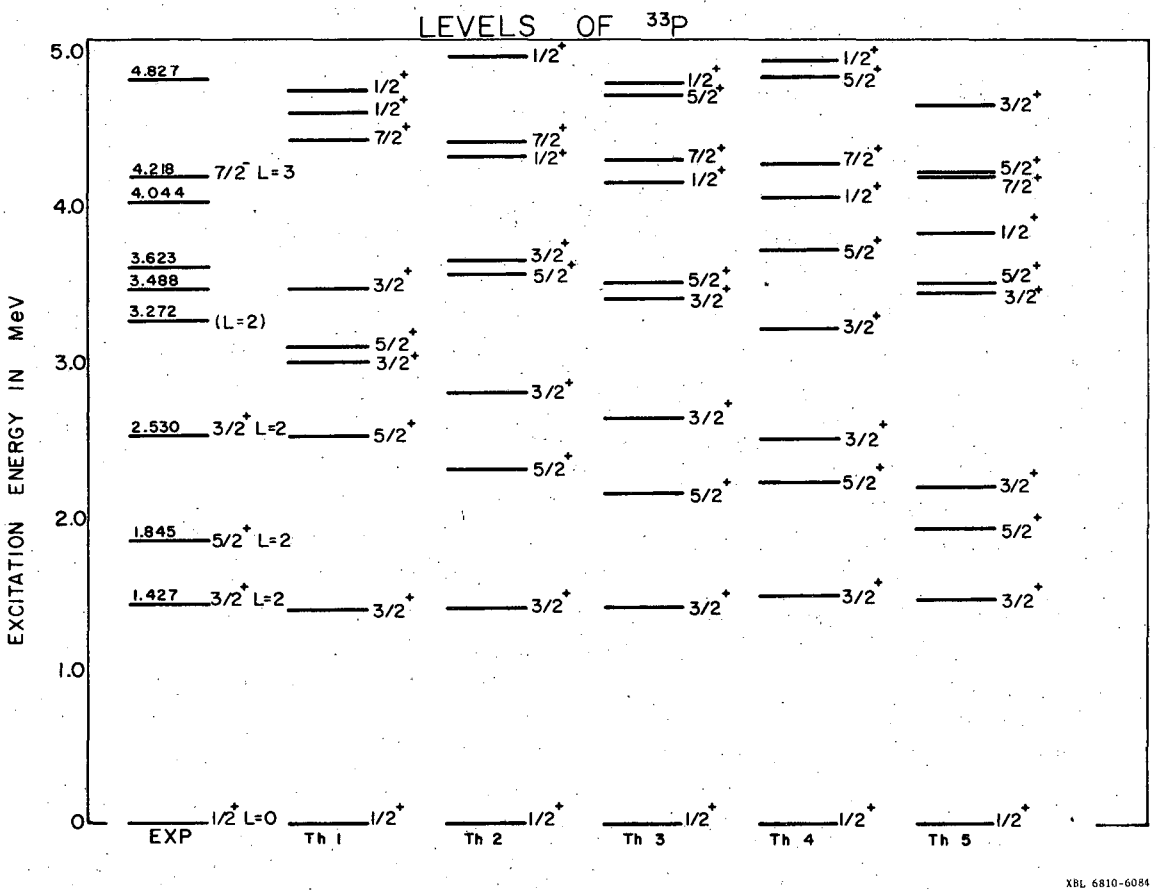
LEVELS OF ^{33}P
EXCITATION ENERGY IN MeV
5.0
4.0
3.0
2.0
1.0
0
4.827
4.218 7/2⁻ L=3
4.044
3.623
3.488
3.272 (L=2)
2.530 3/2⁺ L=2
1.845 5/2⁺ L=2
1.427 3/2⁺ L=2
1/2⁺ L=0
EXP
Th 1
Th 2
Th 3
Th 4
Th 5
XBL 6810-6084

Fig. 3.

TECHNICAL INFORMATION DIVISION
LAWRENCE RADIATION LABORATORY
UNIVERSITY OF CALIFORNIA
BERKELEY, CALIFORNIA 94720